


RESEARCH

Open Access



# Synthesis of novel isoxazole–carboxamide derivatives as promising agents for melanoma and targeted nano-emulgel conjugate for improved cellular permeability

Mohammed Hawash<sup>1\*</sup> , Nidal Jaradat<sup>1</sup>, Ahmad M. Eid<sup>1</sup>, Ahmad Abubaker<sup>1</sup>, Ola Mufleh<sup>1</sup>, Qusay Al-Hroub<sup>1</sup> and Shorooq Sobuh<sup>2</sup>

## Abstract

**Background:** Cancer is one of the most dangerous and widespread diseases in the world today and it has risen to the position of the leading cause of death around the globe in the last few decades. Due to the inherent resistance of many types of cancer to conventional radiotherapy and chemotherapy, it is vital to develop innovative anticancer medications. Recently, a strategy based on nanotechnology has been used to improve the effectiveness of both old and new cancer drugs.

**Objectives:** The present study aimed to design and synthesize a series of phenyl-isoxazole–Carboxamide derivatives, evaluate their anticancer properties, and improve the permeability of potent compounds into cancer cells by using a nano-emulgel strategy.

**Methods:** The coupling reaction of aniline derivatives and isoxazole–Carboxylic acid was used to synthesize a series of isoxazole–Carboxamide derivatives. IR, HRMS, <sup>1</sup>H-NMR, and <sup>13</sup>C-NMR spectroscopy techniques, characterized all the synthesized compounds. The *in-vitro* cytotoxic evaluation was performed by using the MTS assay against seven cancer cell lines, including hepatocellular carcinoma (Hep3B and HepG2), cervical adenocarcinoma (HeLa), breast carcinoma (MCF-7), melanoma (B16F1), colorectal adenocarcinoma (Caco-2), and colon adenocarcinoma (Colo205), as well as human hepatic stellate (LX-2) in addition to the normal cell line (Hek293T). A nano-emulgel was developed for the most potent compound, using a self-emulsifying technique.

**Results:** All synthesized compounds were found to have potent to moderate activities against B16F1, Colo205, and HepG2 cancer cell lines. The results revealed that the **2a** compound has broad spectrum activity against B16F1, Colo205, HepG2, and HeLa cancer cell lines with an IC<sub>50</sub> range of 7.55–40.85 μM. Moreover, compound **2e** was the most active compound against B16F1 with an IC<sub>50</sub> of 0.079 μM compared with Dox (IC<sub>50</sub> = 0.056 μM). Nanoemulgel was used to increase the potency of the **2e** molecule against this cancer cell line, and the IC<sub>50</sub> was reduced to 0.039 μM. The antifibrotic activities were investigated against the LX-2 cell line, and it was found that our synthesized

\*Correspondence: mohawash@najah.edu

<sup>1</sup> Department of Pharmacy, Faculty of Medicine and Health Sciences, An-Najah National University, Nablus 00970, Palestine

Full list of author information is available at the end of the article



© The Author(s) 2022. **Open Access** This article is licensed under a Creative Commons Attribution 4.0 International License, which permits use, sharing, adaptation, distribution and reproduction in any medium or format, as long as you give appropriate credit to the original author(s) and the source, provide a link to the Creative Commons licence, and indicate if changes were made. The images or other third party material in this article are included in the article's Creative Commons licence, unless indicated otherwise in a credit line to the material. If material is not included in the article's Creative Commons licence and your intended use is not permitted by statutory regulation or exceeds the permitted use, you will need to obtain permission directly from the copyright holder. To view a copy of this licence, visit <http://creativecommons.org/licenses/by/4.0/>. The Creative Commons Public Domain Dedication waiver (<http://creativecommons.org/publicdomain/zero/1.0/>) applies to the data made available in this article, unless otherwise stated in a credit line to the data.

molecules showed better antifibrotic activities at 1  $\mu$ M than 5-FU, and the cell viability values were 67 and 95%, respectively.

**Conclusion:** This study suggests that a **2e** nano-formalized compound is a potential and promising anti-melanoma agent.

**Keywords:** Isoxazole, Anticancer, B16F1, LX-2, Nano, Doxorubicin

## Background

Cancer is a generic word that indicates a large group of about 100 diseases. It can affect any organ in the body and usually occurs when a cell breaks the cell-division restrictions, causing an abnormal proliferation and growth of the cells [1]. In addition to the genetic factor, there are plenty of environmental factors that contribute to the development of different types of cancer, such as high consumption of tobacco and alcohol, a low level of physical activity, exposure to radiation, and viral infection [2–4].

Up until now, cancer has been one of the most lethal common diseases and is the second leading cause of death worldwide [5, 6]. In 2020, 19.3 million new cases were estimated to have cancer, with about 10.0 million deaths [7]. According to recent World Health Organization (WHO) posts, the percentage of common cancer types was 2.26 million in the breast, 2.21 million in the lung, 1.93 million in the rectum and colon, 1.2 million in the skin, and about 1 million in the liver [1, 8].

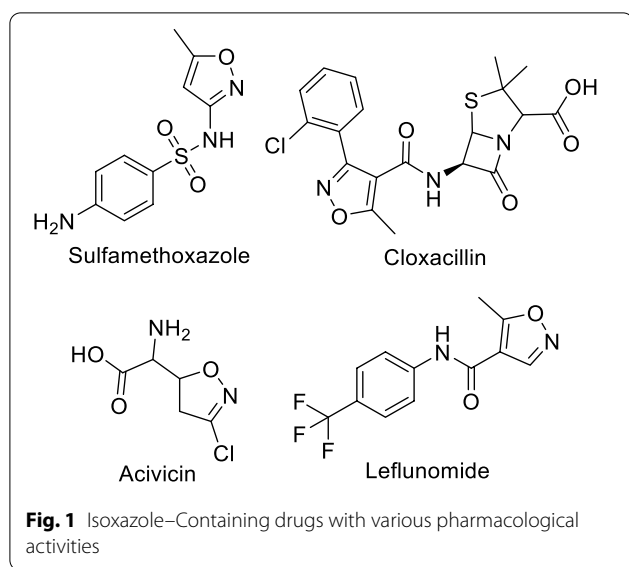
Skin cancer is divided into two types: melanoma is the sixth most common cancer in women and the fifth most common cancer in men [9], and is considered one of the most common types in the United States, where one in every five Americans will have cancer by the age of seventy. Skin color is considered one of the risk factors for melanoma, which is 20 times more prevalent in white people than in black people [10–12]. Early diagnosis of melanoma is a critical point in treatment because it decreases long-term and short-term mortality and morbidity. There is a series of pathways to diagnosis, which first occurs visually by using dermoscopy, then taking a biopsy, and making a histopathological assessment. The melanoma has special architectural features that are different from those in a normal cell, which are: a gathering of growth, asymmetrical in shape, and outstanding nucleoli with a thick and unequal nuclear membrane [9, 13, 14]. A lot of strategies are used for treatment, like surgical removal, immunotherapy, and chemotherapy. But the type of treatment used depends on the stage of the tumor [9].

Liver fibrosis is considered the major consequence of pathological hepatic diseases and clinically represents the major complications of the last stage of hepatic disease. As liver fibrosis advances, a large amount of extracellular

matrix (ECM) like collagen is produced and accumulated, which leads to hepatic dysfunction and cirrhosis. The main cellular origin of the extracellular matrix is the hepatic stellate cells (HSC). HSC, in its quiescent state, is considered the main site for the storage of vitamin A, which is necessary for the homeostasis regulation of retinoic acid. When a hepatic injury occurs, the HSC will transform into a myofibroblast-like phenotype. This change is associated with liver fibrosis, which will produce a lot of growth factors, and cytokines, and the ECM will be remodeled. The LX-2 cell line is an unbounded source of human HSC. It has activated HSC features like retinoid metabolism, cytokine signaling, fibrogenesis, and neuronal gene expression [15]. The anti-fibrotic agents usually induce apoptosis via various regulatory pathways, including the mitochondrial-induced apoptosis members of the bax and bcl-2 families, and phosphorylated mitogen-activated protein kinases, containing c-Jun N-terminal, extracellular (EC) signal-regulated kinases and p38 protein [15, 16].

Chemotherapy is still an essential therapy in most cancer types, whether it is used alone or in conjunction with another strategy of treatment [6, 17]. In recent decades, a lot of studies have aimed to make novel chemotherapeutic drugs, by making modifications to existing ones [18, 19], or isolating compounds from plants [20].

A lot of heterocyclic compounds have anticancer activity, such as isoxazole [18, 21] and pyrazole [22–25]. Recently, numerous studies have been conducted on heterocycles such as isoxazole, pyrazole, and thiazole derivatives as pharmacologically active agents [26–32]. Heterocyclic isoxazole is a 5-membered ring containing three carbon atoms, a nitrogen atom, and an oxygen atom adjacent to each other [33, 34]. They found that it had anticancer [35–37], antiviral for HIV [38], antimicrobial [39, 40], anti-inflammatory [41, 42], analgesic [39], hypoglycemic [43], and antioxidant activity [33]. Some of these compounds have been approved and become available on the market, like Sulfamethoxazole (Fig. 1) [44] and Cloxacillin (Fig. 1), which have antibacterial activity [45], and Acivicin (Fig. 1), which has anticancer activity [46]. A lot of the synthesized compounds consisted of an aryl group with halogen substitute and a carboxamide linker that bound it with isoxazole group found to have anti-tumor activity, and one of these compounds was



Leflunomide (Fig. 1) which was approved for the treatment of rheumatoid arthritis. Recently, this drug was shown to be antiproliferative against bladder cancer cell lines and can induce cell cycle arrest at the S phase of the cell cycle [47].

To reduce the undesirable side effects of chemotherapy, a new branch of alternative therapeutic approach to more specific targets of cancer cells without harming normal cells has been developed. A nanotechnology strategy has been used recently to enhance the effects of both traditional and new pharmacological anticancer treatments. The latest development in the drug delivery field is using nanoparticles (NPs) in a more specific way to reach tumor cells. Due to its small size (1 to 100 nm), it accumulates in tumor cells [48].

In our previous work, different series of isoxazole derivatives were synthesized and evaluated as anticancer agents, and generally, isoxazole-Carboxamide derivatives exhibited moderate to potent antiproliferative activities against panel cancer cell lines with low values of  $IC_{50}$ s [18, 49]. The current study aims to synthesize a novel 5-methyl-3-phenylisoxazole-4-Carboxamide with several substituents and evaluate its antiproliferative activities against various kinds of cancer cell lines, including B16-F1, Colo205, HepG2, CaCo-2, HeLa, Hep3B, MCF-7, and normal hepatic LX-2 and kidney Hek293t cells. In addition to creating a nanoemulgel to boost the potency of the most active compound on B16-F1.

## Methods

### Chemistry

All used chemical reagents and starting materials were ordered from Alfa Aesar (UK) and Sigma-Aldrich

(Germany). All used cancer, and normal cell lines were ordered from ATCC. The SMP-II Digital Melting Point Apparatus was used without correcting to find the melting points (M.P.) of all final compounds.  $^1\text{H-NMR}$  and  $^{13}\text{C-NMR}$  spectra were recorded by using  $\text{DMSO-d}_6$  as the solvent and were conducted by the Bruker 500 J MHz-Avance III High-Performance Digital FT-NMR spectrometer at the Chemistry department, Science Faculty, in the University of Jordan, Amman-Jordan. However, the chemical shifts were recorded accordingly as  $\delta$  (ppm). The used mass instrument was the High-resolution mass spectrometer (HRMS) at the Pharmaceutical chemistry department, Pharmacy Faculty in Gazi University, Ankara-Turkey, this instrument uses the Waters LCT Premier XE Mass Spectrometer which is coupled to an AQUITY Ultra Performance Liquid Chromatography (UP-LC) system (Waters Corporation, Milford, MA, USA) [50].

### The general synthesis procedure of phenyl-isoxazole-Carboxamide derivatives (2a-2f)

The 5-(methyl)-3-phenyl-1,2-isoxazole-4-Carboxylic acid (compound 1) (609.60 mg, 3 mmol) was dissolved in 20 ml of dichloromethane (DCM), followed by the addition of di methylamino-pyridine (DMAP; 73.30 mg, 0.6 mmol), and  $N'$ -ethyl carbodiimide hydrochloride (EDC; 632.61 mg, 3.30 mmol). Then the mixture was stirred under argon inert gas at room temperature for 30 min, and the aniline derivatives (3.2 mmol) were added. The reactions were monitored by thin-layer chromatography (TLC). After that, the solvent was removed under vacuum pressure and dissolved again in DCM, then extracted with HCl (2 N) to remove any excess aniline derivatives. The organic layer was dried over  $\text{Na}_2\text{SO}_4$  and evaporated under reduced pressure. The obtained final products were purified by flash chromatography using the convenient solvent systems (DCM: ethyl acetate and/or n-hexane: ethyl acetate) and/or then purified by recrystallization utilizing the convenient solvent system [18].

### N-(4-Chloro-2,5-dimethoxyphenyl)-5-methyl-3-phenylisoxazole-4-Carboxamide (2a)

This product was purified by column chromatography using an n-hexane: ethyl acetate (3:2) solvent system, TLC Retention factor of 0.644. Solid product, M.P. 193–195 °C, Yield 67%, 749.35 mg; ESI-MS: 373.0894 (100), 375.0880 (33),  $[M + H]^+$  calcd. 373.0894, found. 373.0955 For  $\text{C}_{19}\text{H}_{17}\text{ClN}_2\text{O}_4$ . IR (FTIR/FTNIR-ATR): 1666.46  $\text{cm}^{-1}$  amide carbonyl (C=O).  $^1\text{H NMR}$  ( $\text{DMSO-d}_6$ )  $\delta$ : 9.20 (1H, s, NH), 7.88 (1H, s, Ar-H), 7.70–7.56 (5H, m, Ar-H), 7.14 (1H, s, Ar-H), 3.79 (3H, s,  $-\text{OCH}_3$ ), 3.64 (3H, s,  $-\text{OCH}_3$ ), 2.67 (3H, s,  $-\text{CH}_3$ ) ppm.  $^{13}\text{C NMR}$  ( $\text{DMSO-d}_6$ )  $\delta$ : 172.41,

160.65, 148.57, 144.75, 130.68, 129.39, 128.86, 128.30, 126.58, 116.74, 113.78, 112.79, 107.94, 56.99, 56.94, 12.83 ppm.

#### 5-Methyl-3-phenyl-N-(3-(trifluoromethyl) phenyl) isoxazole-4-Carboxamide (2b)

This product was purified by column chromatography using DCM: ethyl acetate solvent system (4:1). The TLC retention factor was 0.95. Solid product, M.P. 148–150 °C, Yield 59%, 614.37 mg; ESI-MS: 347.0995 (100), 348.1052 (20),  $[M+H]^+$  calcd. 347.0995, found 347.1007 for  $C_{18}H_{13}F_3N_2O_2$ . IR (FTIR/FTNIR-ATR): 1680.73  $cm^{-1}$  amide carbonyl (C=O).  $^1H$  NMR (DMSO- $d_6$ )  $\delta$ : 10.78 (1H, s, NH), 8.14 (1H, s, Ar-H), 7.83–7.50 (8H, s, Ar-H), 2.63 (3H, s,  $-CH_3$ ) ppm.  $^{13}C$  NMR (DMSO- $d_6$ )  $\delta$  ppm: 170.88 (C=O), 160.91, 160.78, 139.82, 130.61, 130.58, 130.14, 129.33, 128.39, 128.29, 123.77, 120.89, 120.88, 116.28, 116.25, 113.40, 12.46 ( $-CH_3$ ) ppm.

#### N-(4-(2-Methoxyphenoxy) phenyl)-5-methyl-3-phenylisoxazole-4-Carboxamide (2c)

This product was purified by column chromatography using an *n*-hexane: ethyl acetate solvent system (3:2). The TLC retention factor was 0.49. Solid product, M.P. 179–180 °C, Yield 71%, 854.45 mg; ESI-MS: 401.1497 (100), 402.1516 (33),  $[M+H]^+$  calcd. 401.1497, found. 401.1501, for  $C_{24}H_{20}N_2O_4$ . IR (FTIR/FTNIR-ATR): 1677.61  $cm^{-1}$  amide carbonyl (C=O).  $^1H$  NMR (DMSO- $d_6$ )  $\delta$ : 10.40 (1H, s, NH), 7.72 (2H, s, Ar-H), 7.58 (2H, d,  $J=8.5$  Hz, Ar-H), 7.50 (3H, s, Ar-H), 7.17 (2H, t,  $J=9.5$  Hz, Ar-H), 7.02–6.95 (2H, m, Ar-H), 6.85 (2H, d,  $J=8.5$  Hz, Ar-H), 3.76 (3H, s,  $-OCH_3$ ), 2.59 (3H, s,  $-CH_3$ ) ppm.  $^{13}C$  NMR (DMSO- $d_6$ )  $\delta$ : 170.21 (C=O), 160.64, 160.15, 154.51, 151.67, 144.43, 133.63, 130.56, 129.31, 128.57, 128.19, 125.79, 121.86, 121.61, 121.53, 117.03, 113.84, 113.79, 56.08 ( $-OCH_3$ ), 12.36 ( $-CH_3$ ) ppm.

#### 5-Methyl-N-(4-(methylthio) phenyl)-3-phenylisoxazole-4-Carboxamide (2d)

This product was purified by column chromatography using an *n*-hexane: ethyl acetate solvent system (3:2). The TLC Retention factor was 0.66. Solid product, M.P. 144–146 °C, Yield 81%, 789.99 mg; ESI-MS: 325.1008 (100), 326.1086 (20),  $[M+H]^+$  calcd. 325.1008, found. 325.1011, for  $C_{18}H_{16}N_2O_2S$ . IR (FTIR/FTNIR-ATR): 1650.32  $cm^{-1}$  amide carbonyl (C=O).  $^1H$  NMR (DMSO- $d_6$ )  $\delta$ : 10.45 (1H, s, NH), 7.70 (2H, s, Ar-H), 7.60 (2H, d,  $J=7.5$  Hz, Ar-H), 7.50 (3H, s, Ar-H), 7.28 (2H, d,  $J=8$  Hz, Ar-H), 2.59 (3H, s,  $-SCH_3$ ), 2.46 (3H, s,  $-CH_3$ ) ppm.  $^{13}C$  NMR (DMSO- $d_6$ )  $\delta$ : 170.35 (C=O), 160.65, 160.30, 136.50, 133.41, 130.58, 129.31, 128.52, 128.20, 127.54, 120.84, 113.75, 15.94 ( $-SCH_3$ ), 12.38 ( $-CH_3$ ) ppm.

#### 5-Methyl-3-phenyl-N-(4-(trifluoromethoxy) phenyl) isoxazole-4-Carboxamide (2e)

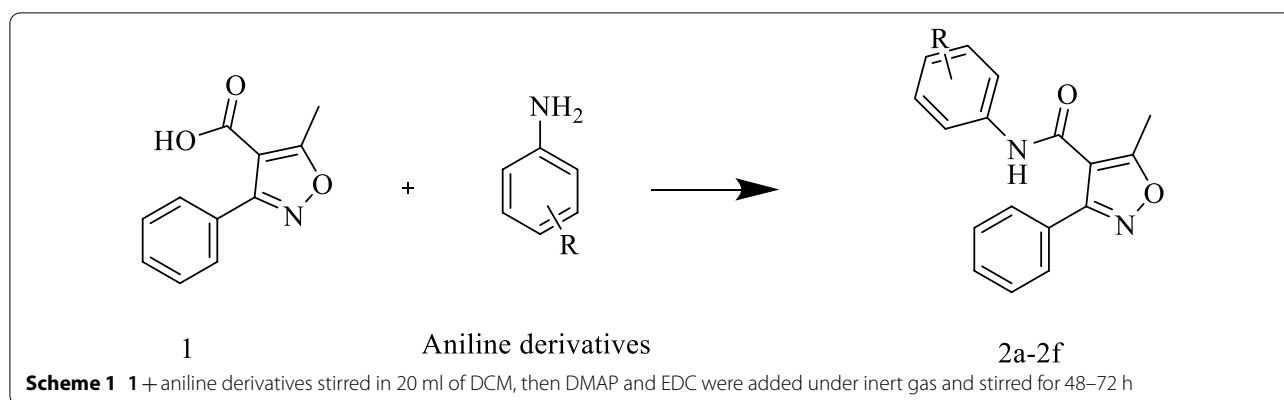
This product was purified by column chromatography using an *n*-hexane: ethyl acetate solvent system (3:2). The TLC Retention factor was 0.69. Solid product, M.P. 158–160 °C, Yield 67.5%, 735.27 mg; ESI-MS: 363.0958 (100), 364.0972 (20),  $[M+H]^+$  calcd. 363.0958, found. 363.0957, for  $C_{18}H_{13}F_3N_2O_3$ . IR (FTIR/FTNIR-ATR): 1659.55  $cm^{-1}$  amide carbonyl (C=O).  $^1H$  NMR (DMSO- $d_6$ )  $\delta$ : 10.66 (1H, s, NH), 7.76 (2H, d,  $J=7.5$  Hz, Ar-H), 7.70 (2H, s, Ar-H), 7.50 (3H, s, Ar-H), 7.37 (2H, d,  $J=8$  Hz, Ar-H), 2.60 (3H, s,  $-CH_3$ ) ppm.  $^{13}C$  NMR (DMSO- $d_6$ )  $\delta$ : 170.59 (C=O), 160.69, 160.61, 155.64, 144.57, 138.26, 130.60, 129.32, 128.43, 128.20, 122.20, 121.60, 113.53, 12.40 ( $-CH_3$ ) ppm.

#### 5-Methyl-3-phenyl-N-(4-(thiophen-2-yl) phenyl) isoxazole-4-Carboxamide (2f)

This product was purified by column chromatography using an *n*-hexane: ethyl acetate solvent system (3:2). The TLC Retention factor was 0.75. Solid product, M.P. 142–144 °C, Yield 79%, 855.79 mg; ESI-MS: 361.0948 (100), 362.0909 (20),  $[M+H]^+$  calcd. 361.0948, found. 361.1011, for  $C_{21}H_{16}N_2O_2S$ . IR (FTIR/FTNIR-ATR): 1650.24  $cm^{-1}$  amide carbonyl (C=O).  $^1H$  NMR (DMSO- $d_6$ )  $\delta$ : 10.56 (1H, s, NH), 7.71–7.47 (11H, m, Ar-H), 7.13 (1H, s, Ar-H), 2.61 (3H, s,  $-CH_3$ ) ppm.  $^{13}C$  NMR (DMSO- $d_6$ )  $\delta$  ppm: 170.46 (C=O), 160.69, 160.41, 143.51, 138.50, 130.60, 130.10, 129.33, 128.92, 128.53, 128.22, 126.37, 125.65, 123.65, 120.60, 113.72, 12.47 ( $-CH_3$ ) ppm.

#### Potent compound nano-emulgel preparation

The nano-emulgel was developed by combining the potent prepared compound nanoemulsions with Carbopol 940 hydrogel. Therefore, the first step was to prepare mineral oil nanoemulsion formulations using a self-emulsifying technique by mixing oil, surfactant (Tween 80), and co-surfactant (Span 80). Then, the optimum nanoemulsion formulation was chosen based on the droplet size and polydispersity index of the mineral oil in the formulation. According to the study, a ternary phase diagram was constructed using various quantities of mineral oil, Tween 80, and Span 80 to determine the optimal nanoemulsion formulation. Each formulation was weighed and vortexed for 2 min. The nanoemulsion was then self-emulsified in distilled water with mild agitation. The size and distribution of the mineral oil and surfactant emulsion droplets were measured using a NanoBrook Omni 280173 (Brookhaven, New York), which also allowed for the determination of the droplet's polydispersity index (PDI) and diameter. Following that, the optimal formulation was chosen to be loaded with the potent compound. It was then combined with



0.4 percent Carbopol 940 hydrogel to create the potent compound nano-emulgel. The PDI, droplet size, and zeta potential were subsequently measured for the obtained nano-emulgel [51].

#### Chemo-informatics parameters of the synthesized compounds

Various websites were used to determine the chemo-informatics characteristic and Lipinski rule of five (RO5) including Molsoft (<http://www.molsoft.com/>) and Molinspiration (<http://www.molinspiration.com/>) [52].

#### Biological methods

##### Cell culture and MTS assay

Hepatocellular carcinoma (Hep3B and HepG2), cervical adenocarcinoma (HeLa), breast carcinoma (MCF-7), melanoma (B16F1), colorectal adenocarcinoma (Caco-2), and colon adenocarcinoma (Colo205), as well as human hepatic stellate (LX-2) in addition to the normal cell line (Hek293T), were used as cancer and normal cell lines and were cultured in RPMI-1640 media and supplemented with 10.0% fetal bovine serum, 1.0% l-glutamine and 1.0% Penicillin/Streptomycin antibiotics. After that, the cells matured in a moist atmosphere with 5.0% CO<sub>2</sub> at 37 °C. In a 96-well plate, the cells were seeded at  $2.5 \times 10^4$  cells/well. After 72 h, the cells were confluent, the media was changed, and then the cells were incubated with various concentrations (300, 100, 50, 10, and 1 μM), as well as lower concentrations (500, 100, and 50 nM) were used, especially for compound 2e against the B16-F1 cancer cell line to calculate accurate IC<sub>50</sub> values for the evaluated compounds (2a–2f) for 24 h. The viability of cells was assessed by the Cell Tilter 96<sup>®</sup> Aqueous One Solution Cell Proliferation (MTS) Assay according to the manufacturer's procedures (Promega Corporation, Madison, WI). However, at the end of the treatment, about 20 μl/100 μl of MTS solution/media was added to each well and for

2 h, they were incubated at 37 °C. Finally, the absorbance was measured at 490 nm [53].

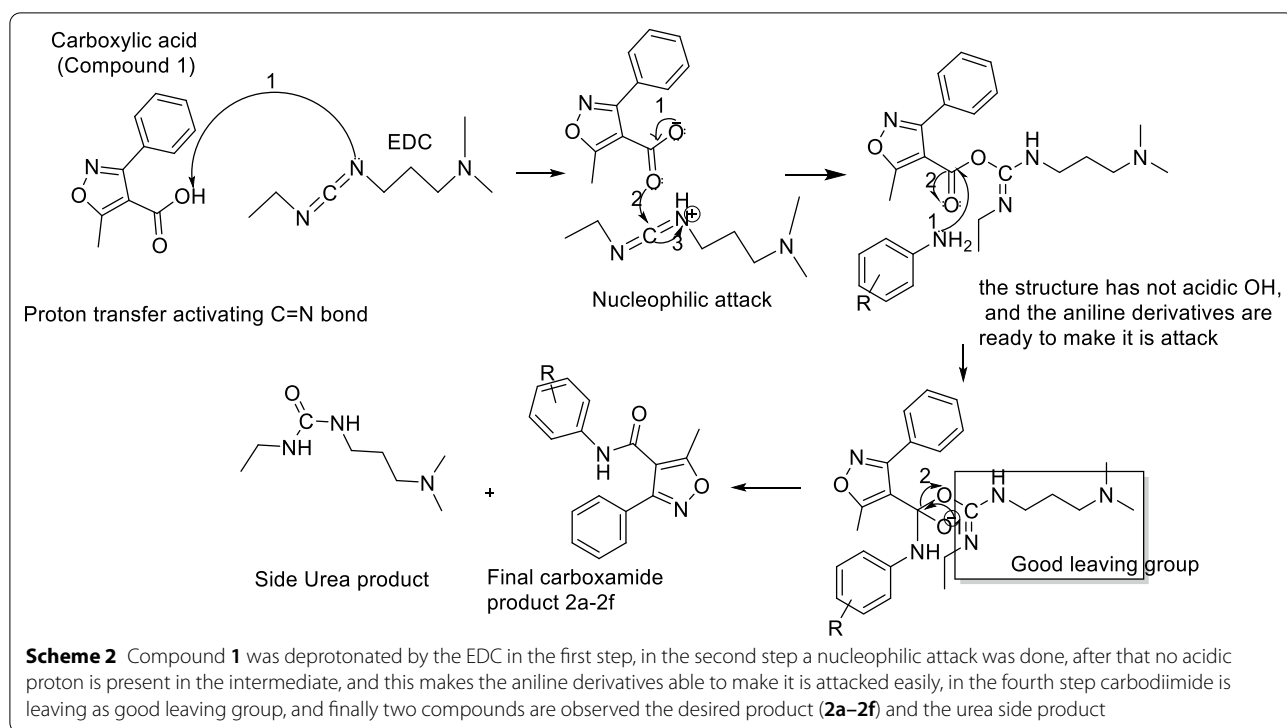
#### Statistical analysis

All of the obtained results were expressed as mean ± SD standard deviation; the result was considered significant when the *p*-value was < 0.05.

#### Results and discussion

##### Chemistry

The synthesis of novel 3-methyl-4-phenyl-isoxazole-Carboxamide derivatives (2a–2f) was presented in “Scheme 1.” The coupling reaction to form the 3-methyl-4-phenyl-isoxazole-Carboxamide compounds (2a–2f) was afforded by using DMAP and EDCI as activating agents and covalent nucleophilic catalysts, respectively. After 30 min, the afforded aniline derivative was added for each reaction [54], the mechanism of this coupling reaction by using the EDC as activating agent is discussed in Scheme 2 [55, 56]. Then each reaction product was purified by column chromatography using different solvent systems (*n*-hexane, ethyl acetate, DCM, and ethyl acetate). The synthesis of these derivatives was confirmed by HRMS and all product masses matched the calculated masses. The yields of all final compounds were in the range of 59–81%, and these results yields seem very close to the previous literature with similar compounds and methods [18, 21, 37, 49]. The observed signals of <sup>1</sup>H-NMR spectrums of the final products showed: firstly, a singlet signal for the proton of amide in ppm range of 9.20–10.78 for all compounds, secondly multiple signals in the aromatic area were observed, then a singlet signal integrated for 3 protons was observed around 2.62 ppm, that should be related to the CH<sub>3</sub> group of Isoxazole ring. Moreover, the main observed signals of <sup>13</sup>C-NMR spectrum showed a clear signal around 170 ppm that should belong to carbonyl carbone, various signals were observed between 160 and 90 ppm for aromatic carbons



as well signal around 12.4 ppm for aliphatic carbon  $\text{CH}_3$  of isoxazole ring.

#### RO5 and chemoinformatics characteristics of the newly synthesized compounds (**2a–2f**)

The chemo-informatic properties were predicted by using computational tools. Results indicate that the newly synthesized products **2a–2f** have good predicted values regarding the polar surface area (PSA;  $\text{Å}^2$ ), molecular weight (g/mol), partition coefficient (log P), hydrogen bond donor, and acceptor (HBD and HBA, respectively). Furthermore, the RO5 tests revealed that almost all of the newly synthesized compounds, **2a–2f**, follow this rule and have excellent values when

compared to the standard (Table 1) [57]. The synthesized products were shown to have good oral bio-availability because all predicted data were within the reference range. Nevertheless, the drug score was calculated and used to assess the synthesized products according to electronic distribution, hydrogen bonding characteristics, flexibility, molecule size, and hydrophobicity, and depending on the results listed in Table 1, showed that most of the synthesized products have good drug scores (0.31–0.61) that define good drug-likeness behavior and may be considered as drug candidate agents versus their targets, except one product (**2b**) showed a bad drug score (– 0.04), which indicates that it does not have good drug-likeness behavior.

**Table 1** Chemo-informatics characteristic of the newly synthesized compounds **2a–2f**

Properties	<b>2a</b>	<b>2b</b>	<b>2c</b>	<b>2d</b>	<b>2e</b>	<b>2f</b>	Standard
M.Wt. (g/mol)	372.09	346.09	400.14	324.09	362.09	360.09	< 500
HBA	5	3	5	4	4	4	< 10
HBD	1	1	1	1	1	1	< 5
Log P	3.70	4.22	4.74	3.78	4.41	4.53	< 5
PSA ( $\text{Å}^2$ )	59.85	45.29	59.75	45.29	51.23	46.04	< 89
nrotb	5	4	6	4	5	4	< 10
Drug Score	0.31	– 0.04	0.50	0.38	0.45	0.61	0.0–2.0

### Potent compound nano-emulgel

Mineral oil nano-emulsion was prepared using a self-emulsifying process. The optimal nanoemulsion was identified for the formulation based on the droplet size and polydispersity index of the mineral oil. As a result, a ternary phase diagram was produced using various quantities of mineral oil, Tween 80, and Span 80 to determine the optimal composition. As shown in Fig. 2, the ternary phase diagram exhibited a significant nano-emulsion zone. Nano-emulsion formulations with droplet size less than 200 nm were chosen. Therefore, the optimum nano-emulsion formulation (35% mineral oil, Tween 80, 50%, and Span 80, 15%) showed the lowest droplet size ( $70.51 \pm 0.5$  nm) and polydispersity index (less than 0.3). As a result, this formulation was loaded with the potent compound and showed a particle size of  $74.28 \pm 0.8$  nm and a polydispersity index of  $0.278 \pm 0.7$ .

The small nanoparticles produced were due to the good oil solubility of the potent compound as it is composed of fatty acids, which helps in developing a formulation with nanoscale particles. In addition to that, the used surfactants were safe, non-ionic (hydrophilic), and biocompatible. By making the surface area large as possible, rapid drug release and absorption were conducted [58]. Moreover, the use of Tween 80 and Span 80 was able to give good emulsification properties to the mineral oil, which helps in producing the nanoparticles [51, 59].

The polydispersity index is critical in determining the stability of the nano-emulgel formulation since it represents the population size distribution within a specific sample. When the polydispersity index is large, the

homogeneity of the particles in the formulation decreases [58]. The polydispersity index of the nano-emulgel formulation is less than 0.3, indicating a narrow and homogeneous globule size distribution and classifying it as a high-stable formulation. A low polydispersity index value indicates a stable nano-emulgel in this investigation [60, 61].

The nano-emulgel stability is also related to its zeta potential. The large negative and positive zeta potential values create a repulsive force between particles, which stabilizes the dispersion. Otherwise, when the zeta potential is low, the dispersion is unstable, which means there is no force keeping the particles apart. Generally, a value of 30 mV or  $-30$  mV is used to denote the stability of dispersions, with values more than 30 mV and less than  $-30$  mV being considered stable systems [59, 62]. As seen in the data, the nano-emulgel had a  $-36 \pm 1.3$  mV value due to the non-ionic surfactants included in the formulation, which covered the system surrounding the surface, assisting in its stabilization. In comparison to particles, they did not affect the stability of the nano-emulsion [63].

### Biological evaluations

#### Cytotoxic evaluation of the compounds 2a–2f

To evaluate the antiproliferative activities of the synthesized compounds, the MTS assay was performed on B16-F1, Colo205, HepG2, Hep3B, CaCo-2, HeLa, and MCF7 cells, as well as the normal cell line, Hek293t. As shown in Table 2, seven concentrations were used (300, 100, 50, 10, 1, 0.5, 0.1 and 0.05  $\mu$ M). Based on the results shown in Table 2, the compound 2a showed a broad range of activities on five cancer cell lines with an  $IC_{50}$  range of 7.54–129.17  $\mu$ M, and this compound was the most potent structure against Colo205 and HepG2 cancer cell lines, with  $IC_{50}$  values of 9.179 and 7.55  $\mu$ M, respectively, as well as potent on normal cell lines Hek293t with an  $IC_{50}$  of 2.54  $\mu$ M. All of the synthesized compounds (2a–2f) showed potent to moderate activities against B16F1 with an  $IC_{50}$  range of 0.079–42.93  $\mu$ M and the most active compound was the 2e compound. In contrast, our synthesized compounds showed weak or negligible activities against Hep3B, CaCo-2, HeLa, and MCF7 cancer cell lines.

Cell viability percentage was calculated for B16F1, Colo205, and HepG2 cancer cells at 50  $\mu$ M concentrations and compared to positive control doxorubicin (Dox) and negative control DMSO, as shown in Fig. 3. The viability percentage for 2a–2d compounds against B16F1 was around 55%, while the percentages were 18.42% and 34.03% for compounds 2e and 2f respectively, in comparison with the dox percentage, which was 21.78%, which means that compound 2e has more

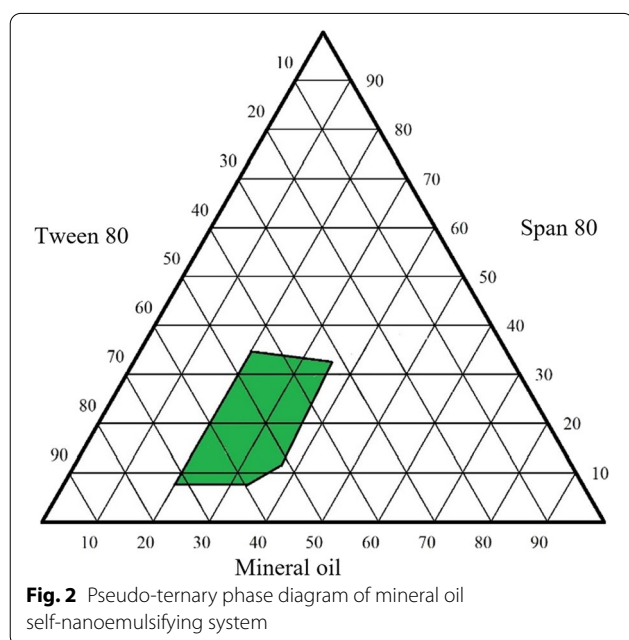
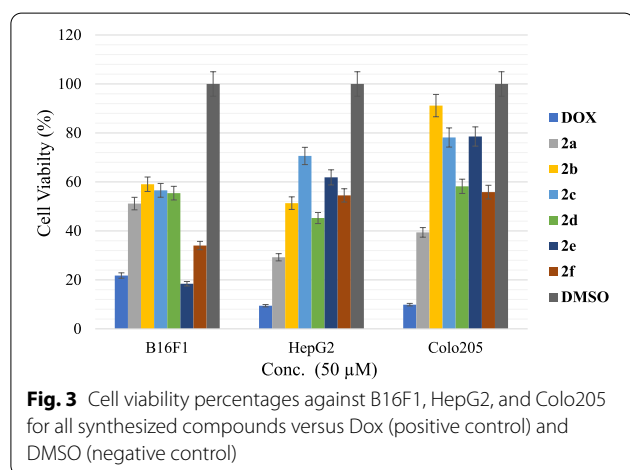
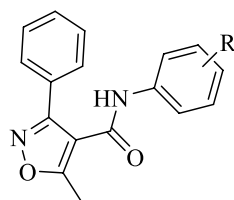


**Table 2** IC<sub>50</sub> (μM) of phenyl-isoxazole–Carboxamide compounds (**2a–2f**) on various cell lines

Code	<b>2a</b>	<b>2b</b>	<b>2c</b>	<b>2d</b>	<b>2e</b>	<b>2f</b>
R	2,5-OMe 4-Cl	3-CF <sub>3</sub>	4-(2-methoxy phenoxy)	4-SCH <sub>3</sub>	4-OCF <sub>3</sub>	4-(thiophen-2-yl)
	IC <sub>50</sub> μM					
Cell line	<b>2a</b>	<b>2b</b>	<b>2c</b>	<b>2d</b>	<b>2e</b>	<b>2f</b>
B16F1	29.72 ± 2.12	42.93 ± 1.55	21.13 ± 0.78	39.84 ± 1.45	<b>0.079</b> ± 0.004	<b>12.72</b> ± 1.01
Colo205	<b>9.18</b> ± 0.88	> 200	183.45 ± 2.05	216.38 ± 1.58	> 200	75.40 ± 2.41
HepG2	<b>7.55</b> ± 0.79	53.58 ± 2.04	120.02 ± 2.19	37.86 ± 2.07	> 200	38.38 ± 1.07
CaCo-2	129.17 ± 2.47	> 200	> 200	> 200	> 200	> 200
HeLa	40.84 ± 1.25	> 200	> 200	> 200	> 200	> 200
Hep3B	> 200	> 200	> 200	> 200	> 200	54.61 ± 2.11
MCF-7	> 200	> 200	> 200	> 200	> 200	> 200
Hek293t	2.54 ± 1.40	147.58 ± 2.74	20.18 ± 1.32	> 200	190.16 ± 2.67	7.91 ± 0.61

*p* value ≤ 0.05



activity against B16F1 in comparison with the positive control (Dox). The cell viability percentage for compound **2a** against HepG2 and Colo205 was 29.24% and 39.39% respectively, in comparison with Dox, values of 9.46% and 9.89%.

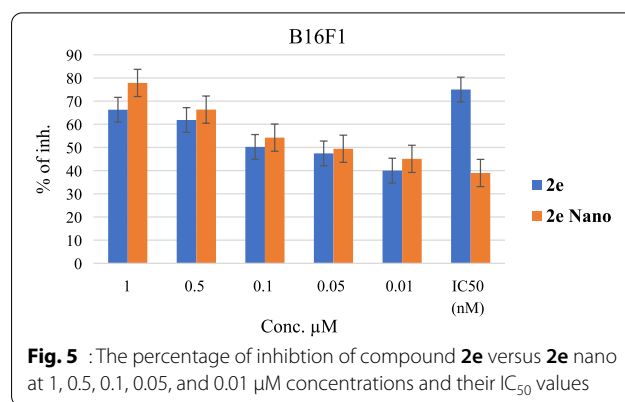
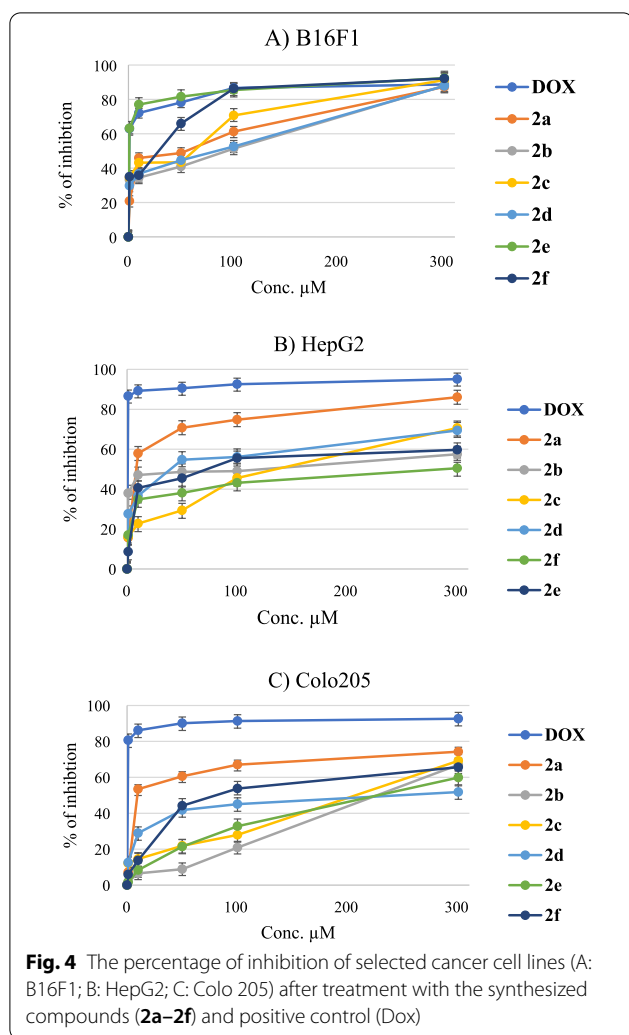
The cell index inhibition percentage was calculated regarding five concentrations (300, 100, 50, 10, and 1 μM) for the selected cancer cell lines (B16F1, HepG2, and Colo205), and presented in Fig. 4. It was clear that the

inhibition percentage of compound **2e** against the B16F1 (Fig. 4A) cancer cell line was very close to the percentage of inhibition of positive control (Dox), and the closest compound against HepG2 and Colo205 to the inhibition percentage of Dox was compound **2a** (shown in Fig. 4B, C).

#### SAR analysis

The isoxazole heterocycle has very important pharmacological activities, especially as anticancer agent according to the recent publications on this core cycle [64], this fact is confirmed as the isoxazole heterocycle could be one of the main pharmacophores for antiproliferative activities, on the other side the activities were better against Hep3B or MCF-7 when the 3-phenyl ring was substituted with halogen (F and/or Cl) [18, 21, 37, 49], while in this study the 3-phenyl ring was unsubstituted and there were very weak activities against these cancer cell lines. Moreover, the substituted groups like CF<sub>3</sub> or OCF<sub>3</sub> on phenyl ring in recent works produced potent anticancer agents [65, 66], especially against melanoma cancer cell line HS27, and this can be confirmed that the most active compound (**2e**) against Melanoma cancer cell line (B16F1) was substituted with OCF<sub>3</sub> group, this group was considered as one of the main pharmacophore sections for anticancer agents [67, 68], as well as when N-phenyl is substituted at





para position with t-butyl substitution showed the most potent activities on cancer cell lines, and this observation was observed previously on our previous works [21, 49].

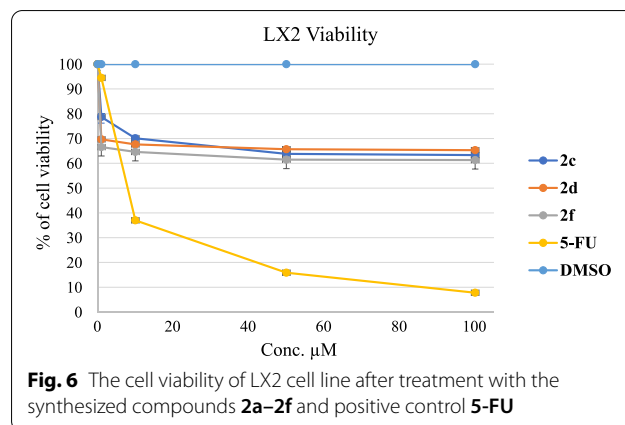
### Nano-emulgel results of compound 2e

The most active compound against the B16F1 cancer cell line was the 2e compound with an IC<sub>50</sub> of 79 nM, and to increase its potency against this cancer cell line, nano-emulgel of this compound was used at 1, 0.5, 0.1, 0.05, and 0.01 μM concentrations and compared the standard compound without nanoemulgel. The results showed that the IC<sub>50</sub> values of nano-emulgel for the 2e compound were decreased to 39 nM in comparison with the standard 2e compound, which was 79 nM. This means that the nanoemulgel increased the potency of this compound fold more than the standard compound. Figure 5 showed the increase of the percentage of inhibition in all used concentrations. This result is attributed to the high penetration of the potent compound nano-emulgel, which is

facilitated by the nanoparticles’ tiny size and wide surface area, which enhances the nano-emulgel’s interaction with cancer cell lines [69]. Moreover, nano-emulgel increased the intracellular uptake of the anticancer agent, which led to an increase in its therapeutic activity. In addition to that, the increase in intracellular retention also plays an important role in increasing efficacy [70].

### Anti-fibrotic activity

To explore the anti-fibrotic effects of these compounds on human hepatic stellate cell (HSC) line LX-2, the viability of LX-2 cells following various compounds’ treatment was determined by the MTS assay. All compounds showed moderate antifibrotic activities. The most active compounds were selected and presented in Fig. 6. They showed very similar activities. The most potent was compound 2f, and the cellular viability of LX-2 was 66.55% at 1 μM concentration in comparison with the positive control 5-FU cell viability value of 94.64%. The results suggested that these compounds have better antifibrotic activities than 5-FU at 1 μM concentration, and further biological investigation into the LX2 cell line is requested soon.



## Conclusion

The synthesized compounds **2a–2f** showed different activities on B16-F1, Colo205, HepG2, Hep3B, CaCo-2, HeLa, and MCF7 cancer cell lines, ranging from moderate to potent activity compared with 5-FU and Dox anticancer drugs. The most potent compound, **2e**, shows great activity on the B16-F1 cancer cell line, with an  $IC_{50}$  value very close to the Dox value ( $IC_{50}=0.079$  and  $0.056 \mu\text{M}$ , respectively). To increase its activity on this cancer cell, a nano-emulgel was prepared to gain a fold effect, which improved from 79 to 39 nM in the nano form. The antifibrotic activities of the synthesized compounds at low concentrations were better than those of 5-FU. The synthesized compounds, especially in the nano form, could be a promising agent for melanoma cancer and further in vitro and in vivo studies should be conducted in the future.

## Abbreviations

ECM: Extracellular matrix; HSC: Hepatic stellate cells; NMR: Nuclear magnetic resonance; M.P: Melting points; HRMS: High-resolution mass spectrometer; DMSO: Dimethyl sulfoxide;  $IC_{50}$ : Half maximal inhibitory concentration; MCF7: Human breast cancer cell line; HeLa: Human cervix adenocarcinoma cell line; Dox: Doxorubicin; Conc.: Concentration.

## Supplementary Information

The online version contains supplementary material available at <https://doi.org/10.1186/s13065-022-00839-5>.

**Additional file 1.** contain the IUPAC name, chemical structures and NMR spectrums of 2a-2f compounds.

## Acknowledgements

The authors would like to thank An-Najah National University, and Gazi University for their support in chemical analysis.

## Author contributions

MH and NJ, conceived and designed the current study. MH, OM, AA, QA, AE, and SS analyzed the data obtained. This paper was written by MH, OM, AA and QA, and drafted by all authors. All authors read and approved the final manuscript.

## Funding

None.

## Availability of data and materials

All data generated or analysed during this study are included in this published article.

## Declarations

### Ethics approval and consent to participate

Not applicable.

### Consent for publication

The authors of the current work gave constant for publication to Dr. Mohamed Hawash.

### Competing interests

The authors declare that they have no competing interests.

## Author details

<sup>1</sup>Department of Pharmacy, Faculty of Medicine and Health Sciences, An-Najah National University, Nablus 00970, Palestine. <sup>2</sup>Department of Biomedical Sciences, Faculty of Medicine and Health Sciences, An-Najah National University, Nablus 00970, Palestine.

Received: 21 April 2022 Accepted: 7 June 2022

Published online: 24 June 2022

## References

1. Cancer IAfRo. World Cancer Report: Cancer research for cancer prevention. Lyon: World Health Organization. 2020.
2. Chu YH, Tzeng SL, Lin CW, Chien MH, Chen MK, Yang SF. Impacts of micro-RNA gene polymorphisms on the susceptibility of environmental factors leading to carcinogenesis in oral cancer. *PLoS ONE*. 2012;7(6): e39777.
3. Schiller JT, Lowy DR. Virus infection and human cancer: an overview. *Recent Results Cancer Res*. 2014;193:1–10.
4. de Menezes RF, Bergmann A, Thuler LC. Alcohol consumption and risk of cancer: a systematic literature review. *Asian Pac J Cancer Prev*. 2013;14(9):4965–72.
5. Sekhon R, Bhatla N. Gynecological cancer update. *Asian J Oncol*. 2016;02(02):061–2.
6. Hawash M. Highlights on specific biological targets; cyclin-dependent kinases, epidermal growth factor receptors, Ras protein, and cancer stem cells in anticancer drug development. *Drug Res (Stuttg)*. 2019;69(9):471–8.
7. Sung H, Ferlay J, Siegel RL, Laversanne M, Soerjomataram I, Jemal A, et al. Global Cancer Statistics 2020: GLOBOCAN Estimates of Incidence and Mortality Worldwide for 36 Cancers in 185 Countries. *CA Cancer J Clin*. 2021;71(3):209–49.
8. Sung H, Ferlay J, Siegel RL, Laversanne M, Soerjomataram I, Jemal A, et al. Global cancer statistics 2020: GLOBOCAN estimates of incidence and mortality worldwide for 36 cancers in 185 countries. *Cancer J Clin*. 2021;71(3):209–49.
9. Ahmed B, Qadir MI, Ghafoor S. Malignant melanoma: skin cancer-diagnosis, prevention, and treatment. *Crit Rev Eukaryot Gene Expr*. 2020;30(4):291–7.
10. Ousley LE, Gentry R, Short C. Instructional dermatology surface models: a new paradigm in nursing dermatology education. *J Dermatol Nurses' Assoc*. 2021;13(6):309–15.
11. Gordon R, editor. Skin cancer: an overview of epidemiology and risk factors. *Seminars in oncology nursing*; 2013: Elsevier.
12. Susianti S, Lesmana R, Salam S, Julaeha E, Pratiwi YS, Sylviana N, et al. The Effect of Nutmeg Seed (M fragrans) Extracts Induces Apoptosis in Melanoma Maligna Cell's (B16–F10). *Indonesian Biomed J*. 2021;13(1):68–74.
13. Dorrell DN, Strowd LC. Skin Cancer Detection Technology. *Dermatol Clin*. 2019;37(4):527–36.
14. Babino G, Lallas A, Longo C, Moscarella E, Alfano R, Argenziano G. Dermoscopy of melanoma and non-melanoma skin cancer. *G Ital Dermatol Venereol*. 2015;150(5):507–19.
15. Xia Y, Chen J, Cao Y, Xu C, Li R, Pan Y, et al. Wedelolactone exhibits anti-fibrotic effects on human hepatic stellate cell line LX-2. *Eur J Pharmacol*. 2013;714(1–3):105–11.
16. Rangwala F, Williams KP, Smith GR, Thomas Z, Allensworth JL, Lyerly HK, et al. Differential effects of arsenic trioxide on chemosensitization in human hepatic tumor and stellate cell lines. *BMC Cancer*. 2012;12(1):1–11.
17. Huang CY, Ju DT, Chang CF, Muralidhar Reddy P, Velmurugan BK. A review on the effects of current chemotherapy drugs and natural agents in treating non-small cell lung cancer. *Biomedicine (Taipei)*. 2017;7(4):23.
18. Eid AM, Hawash M, Amer J, Jarrar A, Qadri S, Alnimer I, et al. Synthesis and biological evaluation of novel isoxazole-amide analogues as anticancer and antioxidant agents. *Biomed Res Int*. 2021;2021:6633297.
19. Baytas SN, Inceler N, Yilmaz A, Olgac A, Menevse S, Banoglu E, et al. Synthesis, biological evaluation and molecular docking studies of trans-indole-3-acrylamide derivatives, a new class of tubulin polymerization inhibitors. *Bioorg Med Chem*. 2014;22(12):3096–104.
20. Jaradat NA, Al-Iahham S, Zaid AN, Hussein F, Issa L, Abualhasan MN, et al. Carlina curretum plant phytoconstituents, enzymes inhibitory and

- cytotoxic activity on cervical epithelial carcinoma and colon cancer cell lines. *Eur J Integr Med.* 2019;30: 100933.
21. Hawash M, Jaradat N, Bawwab N, Salem K, Arafat H, Hajjousef Y, et al. Design, synthesis, and biological evaluation of phenyl-isoxazole–Carboxamide derivatives as anticancer agents. *Heterocycl Commun.* 2021;27(1):133–41.
  22. Inceler N, Yilmaz A, Baytas SN. Synthesis of ester and amide derivatives of 1-phenyl-3-(thiophen-3-yl)-1 H-pyrazole-4–Carboxylic acid and study of their anticancer activity. *Med Chem Res.* 2013;22(7):3109–18.
  23. Inceler N, Ozkan Y, Turan NN, Kahraman DC, Cetin-Atalay R, Baytas SN. Design, synthesis and biological evaluation of novel 1, 3-diarylpiperazines as cyclooxygenase inhibitors, antiplatelet and anticancer agents. *Med-ChemComm.* 2018;9(5):795–811.
  24. Abu-Hashem AA. Synthesis of new pyrazoles, oxadiazoles, triazoles, pyrrolotriazines, and pyrrolotriazines as potential cytotoxic agents. *J Heterocycl Chem.* 2021;58(3):805–21.
  25. Gomha SM, Salah TA, Abdelhamid AO. Synthesis, characterization, and pharmacological evaluation of some novel thiadiazoles and thiazoles incorporating pyrazole moiety as anticancer agents. *Monatshefte für Chemie—Chemical Monthly.* 2015;146(1):149–58.
  26. Abu-Hashem AA, Fathy U, Gouda MA. Synthesis of 1, 2, 4-triazolopyridazines, isoxazolofuopyridazines, and tetrazolopyridazines as antimicrobial agents. *J Heterocycl Chem.* 2020;57(9):3461–74.
  27. Gomha S, Khalil K, Abdel-Aziz H. Synthesis and anti-hypertensive  $\alpha$ -blocking activity evaluation of thiazole derivatives bearing pyrazole moiety. *Heterocycles.* 2015;91(9):1763–73.
  28. Abdalla M, Gomha S, Abdelaziz M, Serag N. Synthesis and evaluation of some novel thiazoles and 1, 3-thiazines as potent agents against the rabies virus. *Turkish J Chem.* 2016;40(3):441–53.
  29. Abu-Melha S, Edrees MM, Riyadh SM, Abdelaziz MR, Elfiky AA, Gomha SM. Clean grinding technique: A facile synthesis and in silico antiviral activity of hydrazones, pyrazoles, and pyrazines bearing thiazole moiety against SARS–CoV-2 main protease (Mpro). *Molecules.* 2020;25(19):4565.
  30. Gomha SM, Farghaly TA, Sayed AR, Abdalla MM. Synthesis of Pyrazolyl-Pyrazoles and Pyrazolyl-[1, 2, 4]-Triazololo [3, 4-d][1, 5] Benzothiazepines as p53 Activators Using Hydrazonoyl Chlorides. *J Heterocycl Chem.* 2016;53(5):1505–11.
  31. Abdelhamid AO, Gomha SM, El-Enany WA. Efficient synthesis and antimicrobial evaluation of new azolopyrimidines-bearing pyrazole moiety. *J Heterocycl Chem.* 2019;56(9):2487–93.
  32. Gomha SM, Badrey MG. Novel anti-HIV-1 NNRTIs based on a pyrazolo [4, 3-d] isoxazole. *Information Med Chem Commun.* 2014;2014(5):1685–92.
  33. Agrawal N, Mishra P. The synthetic and therapeutic expedition of isoxazole and its analogs. *Med Chem Res.* 2018;27(5):1309–44.
  34. Barmade MA, Murumkar PR, Sharma MK, Yadav MR. Medicinal chemistry perspective of fused isoxazole derivatives. *Curr Top Med Chem.* 2016;16(26):2863–83.
  35. Yong JP, Lu CZ, Wu X. Potential anticancer agents. I. Synthesis of isoxazole moiety containing quinazoline derivatives and preliminarily in vitro anticancer activity. *Anticancer Agents Med Chem.* 2015;15(1):131–6.
  36. Kumar RN, Dev GJ, Ravikumar N, Swaroop DK, Debanjan B, Bharath G, et al. Synthesis of novel triazole/isoxazole functionalized 7-(trifluoromethyl) pyrindo [2, 3-d] pyrimidine derivatives as promising anticancer and antibacterial agents. *Bioorg Med Chem Lett.* 2016;26(12):2927–30.
  37. Hawash M, Kahraman DC, Ergun SG, Cetin-Atalay R, Baytas SN. Synthesis of novel indole-isoxazole hybrids and evaluation of their cytotoxic activities on hepatocellular carcinoma cell lines. *BMC Chem.* 2021;15(1):1–14.
  38. Sysak A, Obmińska-Mrukowicz B. Isoxazole ring as a useful scaffold in a search for new therapeutic agents. *Eur J Med Chem.* 2017;137:292–309.
  39. Govindappa VK, Prabhaskar J, Khattoon BBA, Ningappa MB, Kariyappa AK. Synthesis of 3, 5-diaryl-isoxazole-4–Carbonitriles and their efficacy as antimicrobial agents. *Pharmacy Chemica.* 2012;4(6):2283–7.
  40. Abu-Hashem AA. Synthesis and antimicrobial activity of new 1, 2, 4-triazole, 1, 3, 4-Oxadiazole, 1, 3, 4-thiadiazole, thiopyrane, thiazolidinone, and azepine derivatives. *J Heterocycl Chem.* 2021;58(1):74–92.
  41. Pedada SR, Yarla NS, Tambade PJ, Dhananjaya BL, Bishayee A, Arunasree KM, et al. Synthesis of new secretory phospholipase A2-inhibitory indole containing isoxazole derivatives as anti-inflammatory and anticancer agents. *Eur J Med Chem.* 2016;112:289–97.
  42. Abu-Hashem AA, El-Shazly M. Synthesis of new isoxazole-, pyridazine-, pyrimidopyrazines and their anti-inflammatory and analgesic activity. *Med Chem.* 2018;14(4):356–71.
  43. Kumar C, Veeresh B, Ramesha K, Raj C, Mahadevaiah K, Prasad S, et al. Antidiabetic studies of 1-benzhydryl-piperazine sulfonamide and carboxamide derivatives. *J Applicable Chem.* 2017;6(2):232–40.
  44. Majewsky M, Wagner D, Delay M, Bräse S, Yargeau V, Horn H. Antibacterial activity of sulfamethoxazole transformation products (TPs): general relevance for sulfonamide TPs modified at the para position. *Chem Res Toxicol.* 2014;27(10):1821–8.
  45. Mani SSR, Iyyadurai R. Cloxacillin induced agranulocytosis: A rare adverse event of a commonly used antibiotic. *Int J Immunopathol Pharmacol.* 2017;30(3):297–301.
  46. Conti P, Roda G, Stabile H, Vanoni MA, Curti B, De Amici M. Synthesis and biological evaluation of new amino acids structurally related to the antitumor agent acivicin. *Farmacol.* 2003;58(9):683–90.
  47. Cheng L, Wang H, Wang Z, Huang H, Zhuo D, Lin J. Leflunomide inhibits proliferation and induces apoptosis via suppressing autophagy and PI3K/Akt Signaling Pathway in Human Bladder Cancer Cells. *Drug Des Devel Ther.* 2020;14:1897–908.
  48. Cassano R, Cuconato M, Calviello G, Serini S, Trombino S. Recent advances in nanotechnology for the treatment of melanoma. *Molecules.* 2021;26(4):785.
  49. Hawash M, Jaradat N, Abualhasan M, Amer J, Levent S, Issa S, et al. Synthesis, chemo-informatics, and anticancer evaluation of fluorophenyl-isoxazole derivatives. *Open Chem.* 2021;19(1):855–63.
  50. Jaradat N, Hawash M, Qneibi M, Shtayeh T, Sobuh S, Arar M, et al. The Effect of Novel Negative Allosteric 2, 3-Benzodiazepine on Glutamate AMPA Receptor and their cytotoxicity. *J Mol Struct.* 2022;34:132936.
  51. Eid AM, Istateyeh I, Salhi N, Istateyeh T. Antibacterial activity of Fusidic acid and sodium Fusidate nanoparticles incorporated in pine oil Nanoemulgel. *Int J Nanomed.* 2019;14:9411–21.
  52. Hawash M, Jaradat N, Shekfeh S, Abualhasan M, Eid AM, Issa L. Molecular docking, chemo-informatic properties, alpha-amylase, and lipase inhibition studies of benzodioxol derivatives. *BMC Chemistry.* 2021;15(1):1–10.
  53. Shi M, Ho K, Keating A, Shoichet MS. Doxorubicin–Conjugated immunonanoparticles for intracellular anticancer drug delivery. *Adv Func Mater.* 2009;19(11):1689–96.
  54. Hawash M, Eid AM, Jaradat N, Abualhasan M, Amer J, Zaid AN, et al. Synthesis and biological evaluation of benzodioxole derivatives as potential anticancer and antioxidant agents. *Heterocycl Commun.* 2020;26(1):157–67.
  55. Cammarata CR, Hughes ME, Ofner CM III. Carbodiimide induced cross-linking, ligand addition, and degradation in gelatin. *Mol Pharm.* 2015;12(3):783–93.
  56. Nakajima N, Ikada Y. Mechanism of amide formation by carbodiimide for bioconjugation in aqueous media. *Bioconjug Chem.* 1995;6(1):123–30.
  57. Jadhav PB, Yadav AR, Gore MG. Concept of drug likeness in pharmaceutical research. *Int J Pharm Biol Sci.* 2015;6:142–54.
  58. Eid AM, Issa L, Al-Kharouf O, Jaber R, Hreash F. Development of coriander sativum oil nanoemulgel and evaluation of its antimicrobial and anticancer activity. *Biomed Res Int.* 2021;2021:10.
  59. Eid AM, Hawash M. Biological evaluation of Saffrole oil and Saffrole oil Nanoemulgel as antioxidant, antidiabetic, antibacterial, antifungal and anticancer. *BMC Complement Med Ther.* 2021;21(1):1–12.
  60. Balakumar K, Raghavan CV, Abdu S. Self nanoemulsifying drug delivery system (SNEDDS) of rosuvastatin calcium: design, formulation, bioavailability and pharmacokinetic evaluation. *Colloids Surf, B.* 2013;112:337–43.
  61. Shakeel F, Haq N, Alanazi FK, Alsarra IA. Polymeric solid self-nanoemulsifying drug delivery system of glibenclamide using coffee husk as a low cost biosorbent. *Powder Technol.* 2014;256:352–60.
  62. Arriaga LR, Drenckhan W, Salonen A, Rodrigues JA, Iniguez-Palomares R, Rio E, et al. On the long-term stability of foams stabilised by mixtures of nano-particles and oppositely charged short chain surfactants. *Soft Matter.* 2012;8(43):11085–97.
  63. Salim N, Basri M, Rahman MA, Abdullah D, Basri H, Salleh A. Phase behaviour, formation and characterization of palm-based esters nanoemulsion formulation containing ibuprofen. *J Nanomedic Nanotechnol.* 2011;2(4):1–5.

64. Arya GC, Kaur K, Jaitak V. Isoxazole derivatives as anticancer agent: A review on synthetic strategies, mechanism of action and SAR studies. *Eur J Med Chem.* 2021;221: 113511.
65. Çalışkan B, Sinoplu E, Ibiş K, Akhan Güzelcan E, Çetin Atalay R, Banoglu E. Synthesis and cellular bioactivities of novel isoxazole derivatives incorporating an arylpiperazine moiety as anticancer agents. *J Enzyme Inhib Med Chem.* 2018;33(1):1352–61.
66. Im D, Jung K, Yang S, Aman W, Hah J-M. Discovery of 4-arylamido 3-methyl isoxazole derivatives as novel FMS kinase inhibitors. *Eur J Med Chem.* 2015;102:600–10.
67. Panathur N, Gokhale N, Dalimba U, Koushik PV, Yogeewari P, Sriram D. New indole–isoxazolone derivatives: Synthesis, characterisation and in vitro SIRT1 inhibition studies. *Bioorg Med Chem Lett.* 2015;25(14):2768–72.
68. Mahajan SS, Scian M, Sripathy S, Posakony J, Lao U, Loe TK, et al. Development of pyrazolone and isoxazol-5-One cambinol analogues as sirtuin inhibitors. *J Med Chem.* 2014;57(8):3283–94.
69. Nirmala MJ, Mukherjee A, Chandrasekaran N. RETRACTED ARTICLE: design and formulation technique of a novel drug delivery system for azithromycin and its anti-bacterial activity against *Staphylococcus aureus*. *AAPS PharmSciTech.* 2013;14(3):1045–54.
70. Mulik RS, Mönkkönen J, Juvonen RO, Mahadik KR, Paradkar AR. Transferin mediated solid lipid nanoparticles containing curcumin: enhanced in vitro anticancer activity by induction of apoptosis. *Int J Pharm.* 2010;398(1–2):190–203.

## Publisher's Note

Springer Nature remains neutral with regard to jurisdictional claims in published maps and institutional affiliations.

Ready to submit your research? Choose BMC and benefit from:

- fast, convenient online submission
- thorough peer review by experienced researchers in your field
- rapid publication on acceptance
- support for research data, including large and complex data types
- gold Open Access which fosters wider collaboration and increased citations
- maximum visibility for your research: over 100M website views per year

At BMC, research is always in progress.

Learn more [biomedcentral.com/submissions](https://biomedcentral.com/submissions)

